Supplementary Material

10.6% Efficient Solution-Processed Cu_2ZnSnS_4 Solar Cells via Cation Substitutions and Li Doping

Outman El Khouja[1,2,3,4], Yuancai Gong[3,4*], Alex Jimenez-Arguijo[3,4], Ilhame Assahsahi[1,2], Ivan Caño[3,4], Harris Goniotakis[3,4], Oriol Segura-Blanch[3,4], Alejandro Navarro Güell[3,4], Cristian Radu[1], Lorenzo Calvo-Barrio[5], Sergio Giraldo[3,4], Marcel Placidi[3,4], Zacharie Jehl Li-Kao[3,4], Aurelian Catalin Galca[1,6*], Edgardo Saucedo[3,4,*]

1. *National Institute of Materials Physics, Atomistilor 405A, 077125 Magurele, Ilfov, Romania*
2. *Electronic Engineering Department, Universitat Politècnica de Catalunya (UPC), Photovoltaic Lab – Micro and Nano Technologies Group (MNT), EEBE, Av Eduard Maristany 10-14, Barcelona 08019, Catalonia, Spain*
3. *Barcelona Center for Multiscale Science & Engineering, Universitat Politècnica de Catalunya (UPC), Av Eduard Maristany 10-14, Barcelona 08019, Catalonia, Spain*
4. *Ibn Tofail University, Campus Universitaire, 14000 Kenitra, Morocco*
5. *Scientific and Technological Centers (CCiTUB),Universitat de Barcelona (UB)*
6. *International Center for Advanced Training and Research in Physics, Atomistilor 409, 077125 Magurele, Romania*

Corresponding authors:Yuancai.gong@upc.edu, ac_galca@infim.ro, Edgardo.saucedo@upc.edu,

Materials and Methods

Solution Preparation

The precursor solution of CZCTS films was prepared under ambient conditions using dimethyl sulfoxide (DMSO, Sigma-Aldrich, 99.9%), 2-methoxyethanol (MOE, Sigma-Aldrich, 99.8%), and dimethyl formamide (DMF, Sigma-Aldrich, 99.8%) as solvents. Initially, 3 g of thiourea (Sigma-Aldrich, 99%) was dissolved in 6 mL of the chosen solvent, followed by the addition of 0.9 g of CuCl (Sigma-Aldrich, 99%), AgCl (Sigma-Aldrich, 99%) to form the TU-Cu-Ag precursor solution. In a separate step, 1.3 g of $SnCl_4$ (Sigma-Aldrich, 98%) was dissolved in 6 mL of solvent, after which 0.8 g of $Zn(CH_3CO_2)_2$ (Sigma-Aldrich, 99.99%) and $CdCl_2$ (Sigma-Aldrich, 99.99%) were added to form the Sn-Zn-Cd precursor solution. Both solutions were stirred continuously until fully dissolved, then combined. Finally, varying amounts of $LiClO_4$ (Thermo Scientific, 99%) were introduced into the mixed precursor solution.

Device Fabrication

The precursor solution was deposited onto an SLG/Mo substrate via spin-coating at 3000 rpm for 30 s, followed by an annealing at 320 °C (DMSO, DMF) or 300 °C (MOE) for 3 min. This deposition-annealing process was repeated seven times, resulting in a final film thickness of 1.2–1.5 µm. The precursor film was then placed inside a graphite box (36 cm^3) along with 100 mg of sulfur pellets and subjected to sulfurization in a tubular furnace (total volume: 5000 cm^3). The furnace was ramped to 680 °C at a rate of 20 °C/min and held at this temperature for 20 min to ensure complete sulfur incorporation. Following sulfurization, a 40 nm CdS as electron transport layer was deposited via chemical bath deposition, followed by an i-ZnO (40 nm) and indium tin oxide (ITO, 150 nm) bilayer deposited via RF magnetron sputtering. Finally, a 500 nm Ag electrode was thermally evaporated, and the device area (0.235 cm^2) was defined using mechanical scribing.

Film and device Characterizations

X-ray diffraction (XRD) patterns were recorded using an Empyrean diffractometer (PANalytical) with Cu Kα radiation as the X-ray source. Raman spectra were acquired with a

LabRAM HR Evolution spectrometer (HORIBA), employing a 532 nm laser diode for excitation. Field emission scanning electron microscope (FESEM) Zeiss Gemini 500 equipped with Energy dispersive X-ray (EDX) detector from Bruker was used to reveal the microstructure and chemical composition of the films. XPS measurements have been done with a monochromatic focused X-ray source (Aluminium Kα line of 1486.6 eV) calibrated using the 3d5/2 line of Ag with a full width at half maximum (FWHM) of 0.6 eV. The analyzed area was a circle of 100 µm in diameter, the sample was placed at 45° with respect to the analyzer axis, and the selected resolution for the spectra was 224 eV of Pass Energy and 0.8 eV per step for the general spectra, and 27 eV of Pass Energy and 0.1 eV per step for the high-resolution spectra of the selected elements. Measurements were referenced to the C1s signal, whose binding energy was equal to 284.8 eV in adventitious carbon. For the electrical characterization of the devices, the current-voltage (I-V) characteristics were recorded using a four-probe Keithley 6430 source meter. I-V curves under illumination were obtained using a calibrated AAA solar simulator (G2V) equipped with LED-based illumination, providing a light intensity of 87.8 mW/cm^2 within the 300–1800 nm range equivalent to the standard 1000 mW/cm^2 across the full AM1.5G spectrum. EQE measurements were conducted using the Enlitech QE-R test system, calibrated with Si and Ge photodiodes as references. Room-temperature capacitance–voltage (C–V) measurements were performed using an impedance analyzer (Novocontrol Technologies). A parallel RC circuit model was employed to extract the device capacitance. Based on the C–V data, doping profiles were calculated using the Miller formalism, assuming a relative dielectric permittivity (ε) of 8.6 for CZTS.

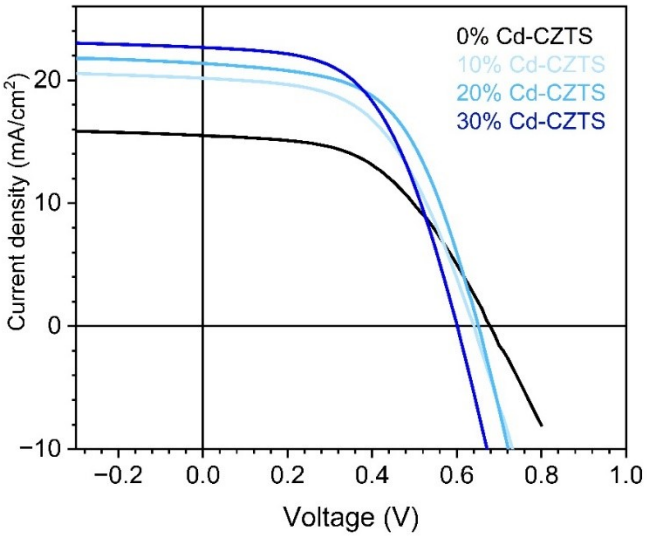

Figure S1. Current density–voltage (J–V) characteristics of CZCTS solar cells using 2-Methoxyethanol solvent with different Cd substitution levels (Cd/(Zn+Cd) = 0, 10, 20, and 30%).

Table S1. Photovoltaic parameters of CZTS solar cells with different Cd substitution levels (Cd/(Zn+Cd) = 0, 10, 20, and 30%)

Device	Voc (mV)	Jsc (mA/cm²)	FF (%)	PCE (%)
0%Cd-CZTS	679	15.05	50.51	5.32
10%Cd-CZTS	641	20.16	52.29	6.76
20%Cd-CZTS	649	21.83	56.05	7.90
30%Cd-CZTS	601	22.66	53.72	7.32

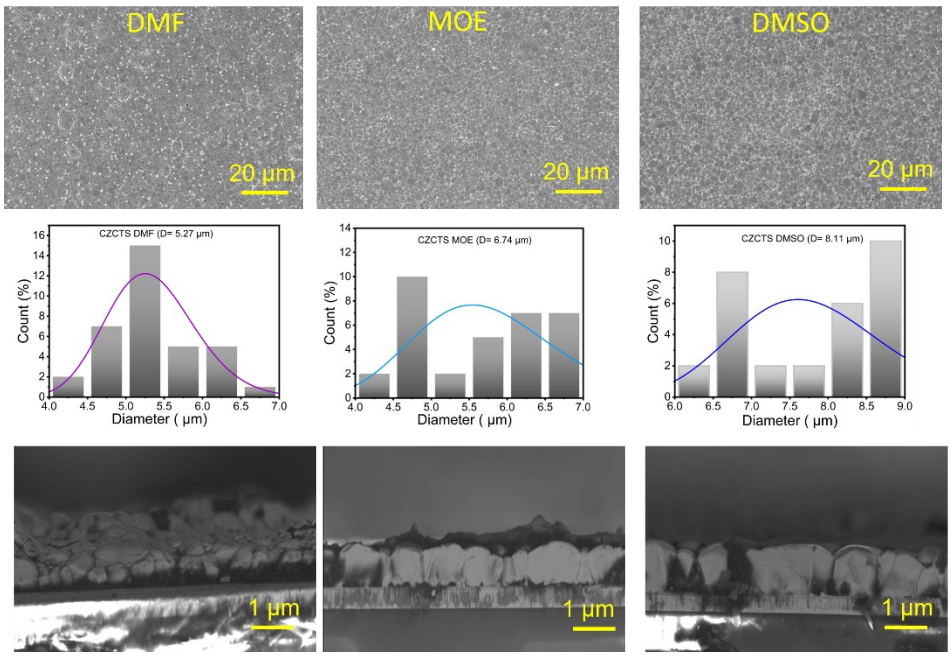

Figure S2. Top view, Size distribution of CZCTS films sulfurized at various temperatures, and Cross-section images for the samples CZCTS prepared with different solvents

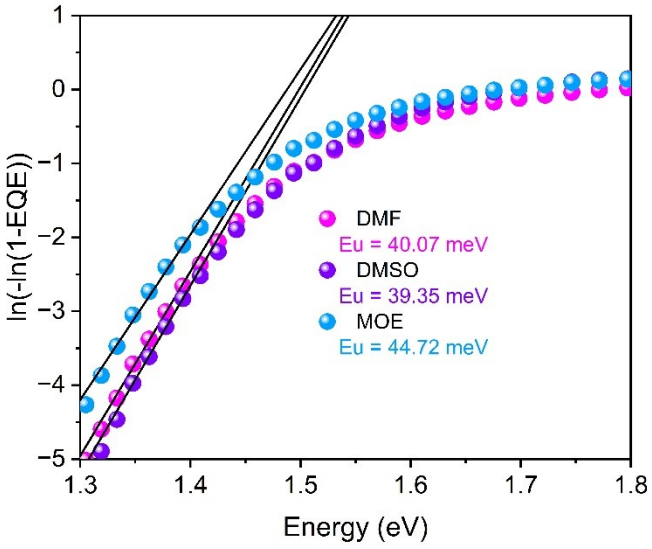

Figure S3. Urbach Energy extracted from the EQE data of the devices fabricated based on the absorber layer prepared with different solvents

To examine the compositional uniformity of the precursor layers before sulfurization, energy-dispersive X-ray spectroscopy (EDX) elemental mapping was performed on the as-deposited CZCTS and ACZCTS films. Figure S4 shows the elemental maps for Cu, Zn, Sn, Cd, and Ag (where applicable). A homogeneous spatial distribution of all constituent elements is observed across the precursor films, indicating effective precursor mixing and the absence of early-stage elemental segregation. This uniformity at the precursor stage is essential for ensuring controlled phase evolution and compositional stability during subsequent high-temperature sulfurization.

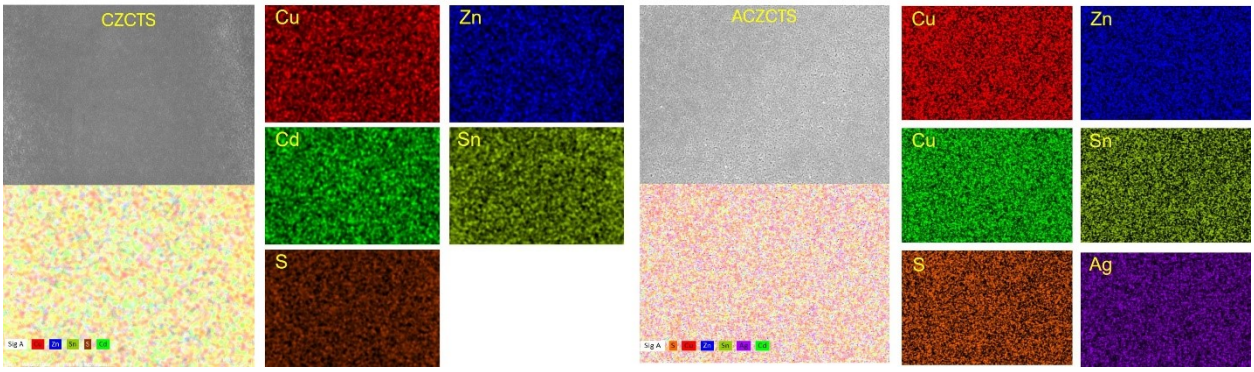

Figure S4. SEM image and corresponding EDX elemental maps of the as-deposited precursor films for CZCTS and ACZCTS, showing uniform spatial distribution of Cu, Zn, Sn, Cd, and Ag before sulfurization

Table S2. Elemental composition of CZCTS and ACZCTS films before and after sulfurization measured by EDX

Sample	State	Cu (at. %)	Zn (.at %)	Sn (at. %)	Cd (at. %)	S (at. %)	Ag (at. %)
CZCTS	As-deposited	23.50	11.11	11.83	3.75	49.80	
CZCTS	Sulfurized	22.11	11.05	10.90	2.60	53.34	
ACZCTS	As-deposited	21.42	12.09	12.34	3.21	48.43	2.51
ACZCTS	Sulfurized	20.73	10.96	11.38	2.10	52.70	2.13

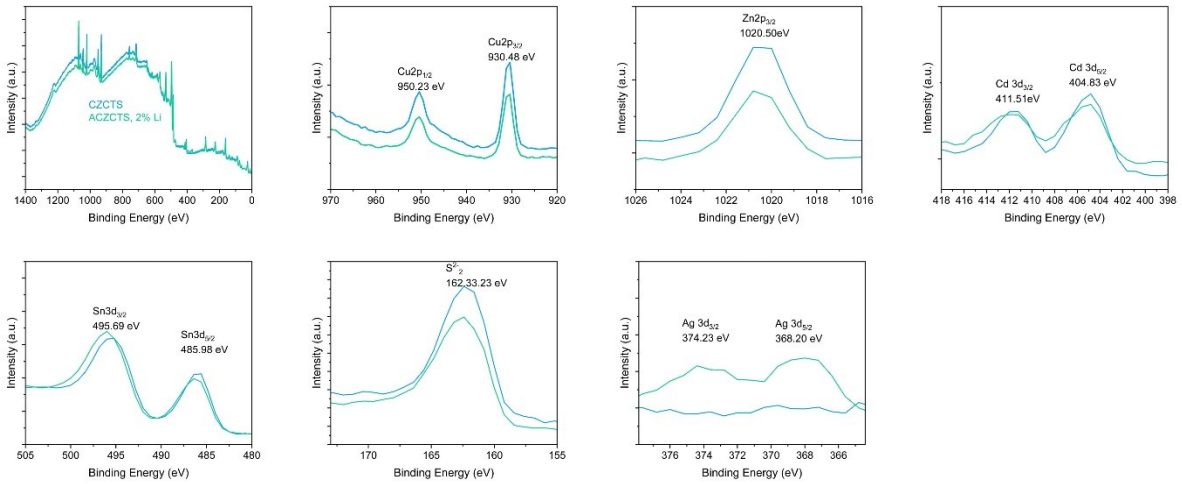

Figure S5. XPS survey and high-resolution core-level spectra of CZCTS and Li-doped ACZCTS absorbers

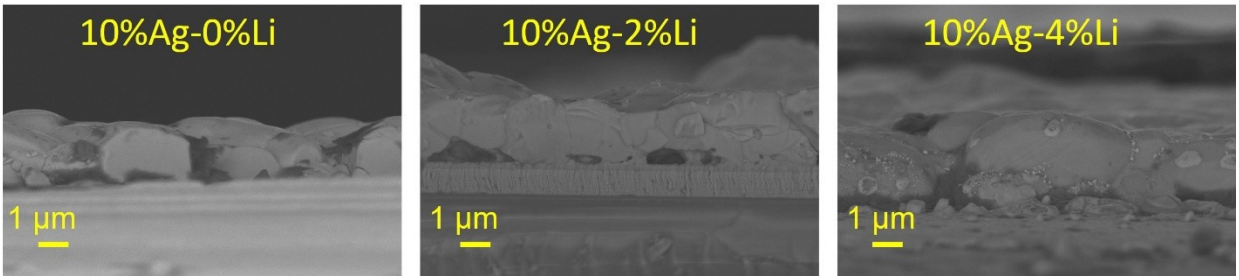

Figure S6. Cross-section images for the samples Li:ACZCTS prepared with different Li doping concentrations

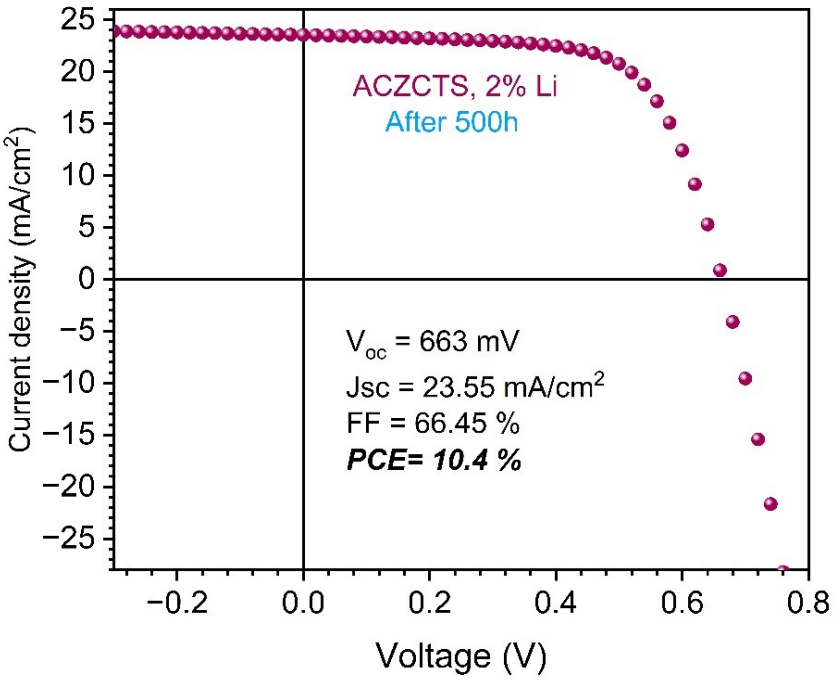

Figure S7. J–V characteristics of the Li:ACZCTS champion device measured after 500 h storage under ambient laboratory conditions